

Dec.2010 / Vol.132

MITSUBISHI ELECTRIC

ADVANCE

Special Issue on Advanced Technologies for Creating Next-Generation Automobiles

• **Editorial-Chief**

Kiyoshi Takakuwa

• **Editorial Advisors**

*Masujima Toshio
Kanae Ishida
Tetsuya Mano
Tetsuji Sorita
Hiroaki Kawachi
Masayuki Masuda
Takahiro Nishikawa
Tetsuyuki Yanase
Ichiro Fujii
Taizo Kittaka
Keiji Hatanaka
Daisuke Kawai
Hideyuki Ichiyama
Toshitaka Aoyagi*

• **Vol. 132 Feature Articles Editor**

Mitsuo Shimotani

• **Editorial Inquiries**

*Tetsuya Mano
Corporate Total Productivity Management
& Environmental Programs
Fax +81-3-3218-2465*

• **Product Inquiries**

*Hideyuki Ichiyama
Automotive Equipment
Fax +81-3-3218-2931*

Mitsubishi Electric Advance is published on line quarterly (in March, June, September, and December) by Mitsubishi Electric Corporation.
Copyright © 2010 by Mitsubishi Electric Corporation; all rights reserved.
Printed in Japan.

CONTENTS

Technical Reports

Overview	1
by <i>Eiji Nakayama</i>	
New Developments in Speech Recognition for Car Navigation System	2
by <i>Yohei Okato and Yuki Furumoto</i>	
High Fidelity Sound Technology for Digital Process Center "DA-PX1"	6
by <i>Kohei Teramoto and Tsuyoshi Nakada</i>	
Third-Generation Power Unit for HEVs	10
by <i>Takuya Michinaka and Yuji Kuramoto</i>	
Estimation of Maximum Tire-Road Friction Coefficient Using Electric Power Assist Steering	13
by <i>Fumiaki Takagi and Noriyuki Inoue</i>	
Model-Based Development of Electronic Control Unit for 4WD	16
by <i>Kazuyuki Adachi and Shinsuke Ui</i>	

Overview



Author: *Eiji Nakayama**

Contribution to the Special Issue on Advanced Technologies for Next-Generation Automobiles

Environment, safety, comfort, cost. These are key words for the design and development of a new generation of automobiles. Mitsubishi Electric's contribution to solving environmental issues includes the mass production of electronic control units for hybrid and electric vehicles, idle stop-start system products, energy regeneration alternators, and electric power steering units. For greater driving safety, control technology for the electric power steering system is used to increase vehicle driving stability. To support safer, more comfortable driving, the car navigation system provides information on traffic jams and merging traffic, as well as route navigation considering traffic congestion. The rapidly expanding auto market in China and India requires small, lightweight vehicles of high quality, but most importantly, low-cost automobile parts. It is therefore necessary to optimize the specifications and utilize locally procured parts, as well as to establish development, production and logistics systems.

The goal of the design and development of a new generation of automobiles is to contribute to a sustainable society; that is, to produce automobiles that are environment friendly, human friendly, and enjoyable to drive. This requires a wide range of sophisticated technologies to be developed. Mitsubishi Electric is proud to contribute its advanced technologies to this important effort.

New Developments in Speech Recognition for Car Navigation System

Authors: *Yohei Okato** and *Yuki Furumoto***

1. Introduction

Mitsubishi Electric is striving to improve speech recognition capabilities for the car navigation system. One of the key problems encountered is when the user speaks out-of-vocabulary words which cannot be recognized. To solve this problem, the speech recognition system was equipped with a smart POI (point of interest) search function⁽¹⁾, which automatically generates variations of each POI name in the recognizable vocabulary. However, along with the expanded vocabulary, both the cost of updating the word variation list and the amount of computation increased. In addition, the same problem has also occurred regarding command and control by voice. Acceptable expressions are limited to those listed in the manual, thus no variations are recognized.

Consequently, we divided the system into two parts: the speech recognition part that converts the input speech into a character string and the post-processing part that performs the text match processing, and we developed a new speech recognition system that avoids an increase in computation when the number of words increases. This paper describes the newly developed speech recognition and post-processing technologies, as well as the voice interface installed in commercial products.

2. Speech Recognition and Post-Processing Technologies

2.1 Speech Recognition Using Statistical Language Model

A language model is a set of data that contains information on the vocabulary to be recognized. The output from the speech recognition process is a sequence of words chosen from the vocabulary registered in the language model so that the word string has the highest likelihood (recognition score) of matching the input speech. Therefore, if the language model contains only the exact name of the point of interest, e.g., "Tokyo National Museum of Modern Art", omitting "National" and using "Tokyo Museum of Modern Art" would not be recognized. Therefore, in the abovementioned smart POI search, the exact name of the POI is divided into separate words: "Tokyo", "National", "Museum", "Modern" and "Art", and then these words along with their conjunction rule are registered in the language model.

For example, by registering the rule that "National" may be omitted, the inexact name "Tokyo Museum of Modern Art" would now be recognized. The drawback of this method is the difficulty related to constructing rules that cover a huge number of variations of POI names, and the resulting high cost.

In contrast, the newly developed speech recognition system employs a statistical language model, where the likelihood of a junction between two words is expressed as a numerical value referred to as the language score. In the case of the POI name, for example, language scores for the word combinations of "Tokyo" followed by "National" and by "Modern" are registered as numerical values, and these language scores are summed up to determine the recognition score of the candidate recognition output. The language score can be automatically generated from a large number of POI names, which reduces the cost of constructing the language model. An additional method was also developed to generate an approximate language score for a word junction containing a word not included in the subject exact name, enabling the recognition of inexact names as well.

However, when the POI name list has several hundred thousand entries, the size of the vocabulary for constructing POI names exceeds a hundred thousand, which is prohibitive for a resource-restricted car navigation system to perform the recognition. Therefore, each word is segmented into smaller element words. For example, "Bijutsu-Kan (Art Museum)" is expressed by the combination of element words, "Bijutsu (Art)" and "Kan (Museum)". The element words are limited to about the top 5,000 words most frequently appearing in POI names. If a word cannot be expressed by a word N-gram, it is expressed by a syllable N-gram. For example, "Kindai (Modern)" is expressed by syllable N-grams: "ki", "n", "da" and "i". Thus, by using the syllable as the base unit of the language model, the vocabulary size can be limited to below a certain level even as the number of POIs to be recognized increases.

2.2 POI Name Search Using High-Speed Text Search Technique

As shown in Fig. 1, the new POI name search system consists of the speech recognition and text match

processes. In the speech recognition part, as described in Section 2.1, each word to be searched is recognized as a sequence of segmented words and syllables. The result of recognition may not have a complete match in the registered vocabulary. In such a case, the text match process searches for a POI name that most closely matches the syllable string given by the recognition process. The score for matching is the number of matched syllable N-grams. An advantage of using the syllable N-gram as the base unit is that the system is more robust to speech recognition errors compared to systems using a word or word N-gram. For example, if "Bijutsukan" (art museum) is erroneously recognized as "Bujutsukan" (martial arts gymnasium), the word-based matching process gives no match results or no score, whereas the syllable-based matching process finds three matching syllable N-grams, "ju-tsu", "tsu-ka" and "ka-n", which are contained in the POI names including "Bijutsukan", and thus contribute to the score. This score can be calculated at high speed by referring to a predetermined inverted index.

2.3 Keyword-based Command and Control System

By using a similar technique to the POI name search, a keyword-based command and control system was developed to increase the rate of acceptability of the user's utterance for a voice command.

Figure 2 shows the process overview of the keyword-based command and control system. The speech recognition part recognizes and converts the input speech to a word string. Based on the keywords contained in the recognition result, the text match part calculates the score for each sentence stored in the text corpus. Each sentence corresponds to a certain command, and the command that is given the highest score is output from the system. In the case shown in Fig. 2, the input speech "Are there any convenience stores near here?" is recognized by the system; then the text match part calculates the score considering the length of contained keywords. In this example, the command "local POI search (convenience store)" is given the highest score and thus is selected as the output. Since

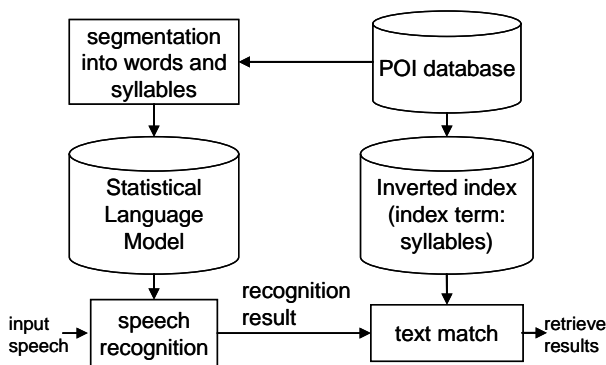


Fig. 1 Overview of POI name search system

this text match process is performed based on the keywords, a certain command can be deduced even if an additional expression is uttered (e.g., polite expressions such as "please do ..."), a particle(s) is omitted, or the word order is changed, thus achieving wider acceptability compared with the conventional system.

Meanwhile, when using the statistical language model that learns from the corpus of commands and controls, an utterance outside the vocabulary is more likely to be misunderstood as a command. In the preliminary study, while a navigation map screen was being displayed, 80% of the utterances outside the vocabulary were POI names. Therefore, for rejection purposes, a sequence of keywords and syllables that frequently appear in POI names was added to the learning data of the statistical language model. In addition, when a keyword of a certain POI name is detected, a special command is output to announce the detection of the POI name. This sequence realizes the POI rejection on the map screen, which is described later.

3. Application to Commercial Car Navigation System (NR-HZ001 Series)

This section describes the voice interface of the HDD car navigation system, to which the above described speech recognition and post-processing technologies are applied.

3.1 Kana Input Based POI Search by Voice

The kana input based POI voice search system searches for the POI name given as voice input. The system enables extremely fast input of any POI name and greatly enhances user convenience compared with character-by-character manual input using a kana keypad, as shown in Fig. 3.

By touching the "Push-to-Talk" button shown in Fig. 3, the search system is activated. Figure 4 shows the results screen when the user's utterance "Sukaibiru" (Sky Building) is recognized and a search is performed on the POIs within Osaka Prefecture. The speech recognition result "Sukaibiru" is displayed (simultaneously, speech output is also provided). Forty-eight candidates

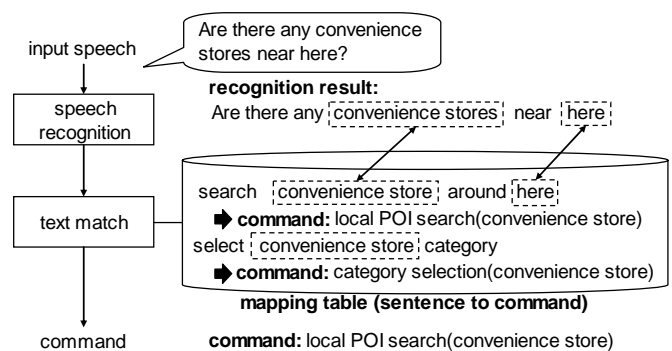


Fig. 2 Overview of keyword-based command and control

that contain “Sky Building” in their names were retrieved from the POIs within Osaka Prefecture, and some of the 48 facilities are listed on the screen. At this stage, the user can either choose the requested POI by manual operation or by uttering “Next” or “Previous”; or the user can utter an additional POI name to narrow down the candidates.

3.1.1 Expansion of POI Search Range and Search by Prefecture

The conventional POI voice search covered a smaller number of POIs than the manual input search. Therefore, some POIs could not be found by voice search, which made users distrustful of the POI voice search.

In response, the kana input based POI voice search was constructed to cover ten million POIs throughout Japan, the same level as for the manual input POI search. However, if all POIs are subjected to the search, too many POIs having the same or similar name will be found, resulting in the additional difficulty of pinpointing the desired POI.

As a solution, we limited the range of search to one prefecture at a time (maximum one million POIs) and prepared an operation screen for switching the prefecture to be searched. By limiting the number of POIs to be searched, the new system offers greater search accuracy and speed.

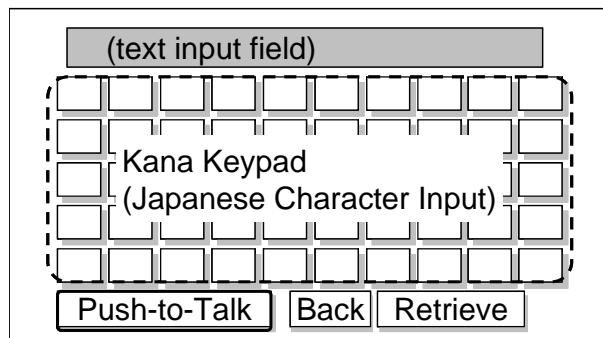


Fig. 3 “Kana” keypad screen for POI search

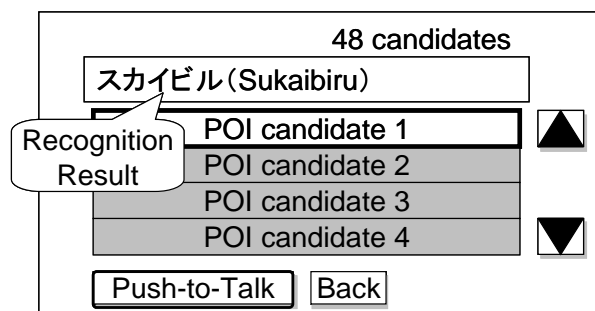


Fig. 4 Search results screen

3.1.2 Display of Speech Recognition Results

There are mainly two cases when the voice search does not operate satisfactorily as expected by the user:

1) the speech recognition ends up with erroneous results, which leads to the wrong search results; 2) both the speech recognition and POI search work properly, but the desired POI is not included in the POI entries subjected to the search.

The newly developed kana input based POI voice search system employs text search technology that is robust to recognition errors, as described in Section 2.2, and thus the problems in category 1) are significantly reduced. In contrast, the problems in category 2) are due to the POI database and it is basically impossible to retrieve the POI called on by the user.

To help the user distinguish between 1) and 2), the recognition results are displayed and the operation guide is provided in response to the user’s utterance (Fig. 4). With this help, the user is able to properly determine the next action according to the result of the voice search (retry the search, narrow down the search results, etc.).

3.2 Rejection of Out Of Vocabulary Words on Map Screen

The car navigation speech recognition system contains the vocabulary as the recognition target according to the display screen and other situations. However, the user is not aware of the contents of the vocabulary and often utters a word not included in the vocabulary, which is not properly recognized and hence, navigation is not provided as expected by the user. This led to users’ complaints about operation by voice.

As a solution, current commercial models (2009 autumn models and later) are equipped with a function for POI rejection on the map screen, which applies a keyword-based command and control system. If the system detects the user’s utterance of a POI name made on the screen where the POI voice search is not active, it informs the user that the POI name will be recognized on the kana input based POI search screen. With this function, a user who is looking for a certain POI can be guided to the screen for the kana input based POI voice search.

4. Conclusion

We have presented some of the latest developments in speech recognition capabilities for car navigation systems, where new features have been realized by combining the speech recognition and post-processing functions. Although the voice is the most natural human interface for input, speech recognition by itself is merely an input means. For improved operability of the car navigation system, as described in this paper, speech recognition must be combined with post-processing to realize highly functional features. We intend to continue working on a voice help system by integrating the semantic understanding and dialog

control functions, and the intellectual information retrieval and display system in combination with the estimated user favorites.

References

- (1) Iwasaki, Kosaka, Nanba and Narita: "Voice Interface of Car Navigation System – Current Technologies and the Future", Mitsubishi Denki Giho, pp. 51–54 (Sep. 2004)
- (2) Hanazawa, Okato and Iwasaki: "Large Vocabulary Spoken Query Retrieval Based on Speech Recognition Using Statistical Language Model and Text Match", Proceedings of 2009 Autumn Meeting of Acoustical Society of Japan, pp. 61–62 (Sep. 2009)

High Fidelity Sound Technology for Digital Process Center “DA-PX1”

Authors: Kohei Teramoto* and Tsuyoshi Nakada*

1. Introduction

DIATONE DA-PX1 delivers excellent sound quality for in-car audio thanks to Mitsubishi Electric’s own audio technologies. Our development target was to improve high-fidelity sound beyond that of a home system. The key technology is the DIATONE original D/A converter for high-precision conversion of digital signals from CDs, USBs (universal serial bus), and other sound sources. We enhanced the precision of the clock signal and reduced the digital noise; we implemented our own jitter reduction circuit and differential transmission in equipment wherever applicable to make the system impervious to data transmission noise; we introduced our own original method for volume control without sound deterioration; and took other measures to achieve a superior digital audio sound. In addition, for sound compensation and higher audio quality in the automobile environment where loudspeakers cannot be arranged in the ideal position, we also implemented many of our own technologies.

This paper describes the high-precision D/A converter and other high fidelity sound technologies.

2. System Configuration

As shown in Fig. 1, the system consists of four units: the main unit with built-in digital-analog selector, A/D (analog to digital) converter, digital signal processor

(DSP), and D/A converter; a satellite unit with built-in memory player having two USB ports; a display unit with independent display screen; and a compact remote controller.

3. High Sound Quality D/A Conversion Technology

We paid special attention to the D/A conversion technology, which is the heart of the DA-PX1. It is not easy to reproduce the aspect of music that most engages the listener: the spatial and stereo impression as if actually seeing the movement of the singer’s lips. The loss of this aspect through the slightest inattention to detail reflects the sensitivity of the audio world. The key to successful digital audio lies in the D/A conversion technology; only by thoroughly improving the digital signal transmission and persisting toward higher-precision D/A conversion is it possible to hear the “engaging aspect” that is normally buried. The perfect Milky Way of sound gradually becomes audible, just like the night sky in the city changes to a clear, star-filled sky high up in the mountains, drawing you in.

To reproduce this aspect, DIATONE has to satisfy the following three conditions simultaneously: (1) the D/A converter must have ultra high precision and be impervious to digital noise; (2) any jitter or digital noise from the digital signal processor must be blocked from

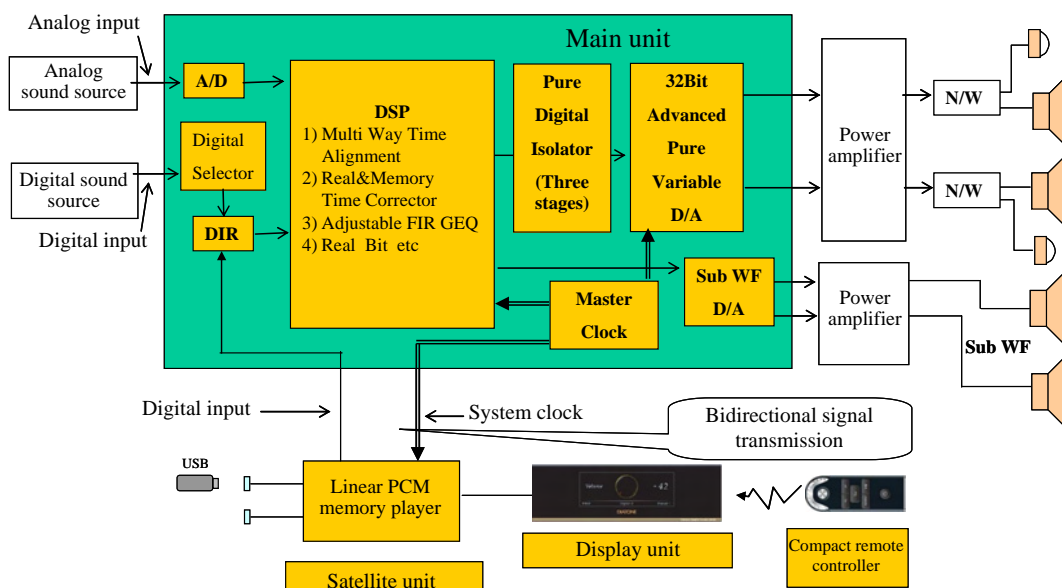


Fig. 1 System configuration

being transmitted into the D/A converter; and (3) the clock must not be affected by external disturbances and must maintain high precision. To satisfy these conditions, we developed the following three new technologies.

3.1 32-bit Advanced Pure Variable Current D/A Converter

In 1991, Mitsubishi Electric commercialized the digital AV center "DA-P7000" equipped with a pure variable current D/A converter. The new 32-bit advanced version has further reduced the influence of jitter, enhanced the precision, and realized current-to-voltage conversion without using an amplification circuit.

The principle of the pure variable current D/A converter is schematically shown in Fig. 2. In this converter, an analogous mechanical relay is capable of operating at ultra high speed (it is actually an ECL (emitter-coupled logic) current switch); and the relay is controlled to open or close by one-bit DAC (digital-to-analog conversion) signals generated by the DAC driver. Meanwhile, an extremely clean constant current source is prepared. This current is switched on or off by the relay, and the switched current is converted to an output voltage. Even if noise from the power source or ground line is superimposed on the output signal of the

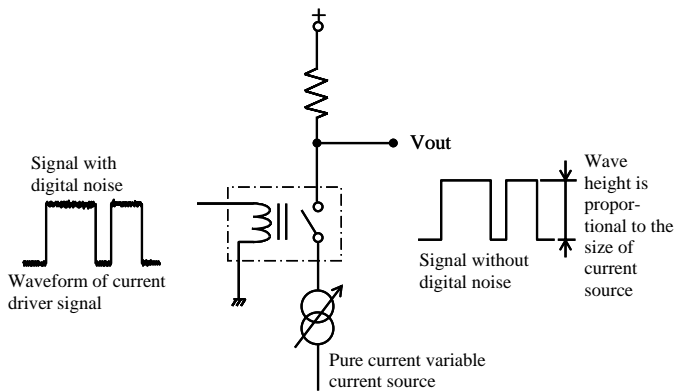


Fig. 2 Principle of pure variable current D/A converter

DAC driver, it has no effect at all on the stage beyond the relay as long as the open and close timing maintains its accuracy. The wave height of the one-bit DAC depends on the constant current source, and hence any effect from external disturbances can be eliminated by making this constant current source clean. In addition, by varying the current level of the constant current source, the wave height can be controlled. Therefore, the pure variable current D/A converter works by itself as a volume controller without generating any bit loss as in the case of digital volume control, thus achieving high sound quality without any information loss even at a very low volume.

The newly developed 32-bit advanced pure variable current D/A converter consists of a DAC driver and DAC signal generation unit. The DAC driver was custom designed using a field-programmable gate array (FPGA), and generates one-bit on/off control signals with 32-bit accuracy. The fifth-order noise shaper and 32-bit level quantizer generate two complementary signals. Meanwhile, as shown in Fig. 3, the DAC signal generation unit is equipped with a pair of equivalent ultra-low-noise current sources and two sets of ECL high-speed current switches. Each of the ECL current switches is on/off controlled by the DAC driver. During no-signal periods, the complementary control signal circuit provides a pair of 50% duty cycle and reversed phase signals, and thus the resultant current from the two ECL current switches remains completely constant. Therefore, even if a jitter is superimposed on the 50% duty cycle signals and the duty cycle is disturbed, the jitter components are cancelled out and do not appear in the output signal, resulting in reduced waveform distortion as low as 1/16. The reference current source was thoroughly "purified", by eliminating external disturbances coming through various routes including the power supply, ground line and vibration. In addition, by varying the current level of this constant current source, linear volume control has been achieved down to -80 dB. For the current-to-voltage conversion of the resultant current after passing through the ECL switches, a

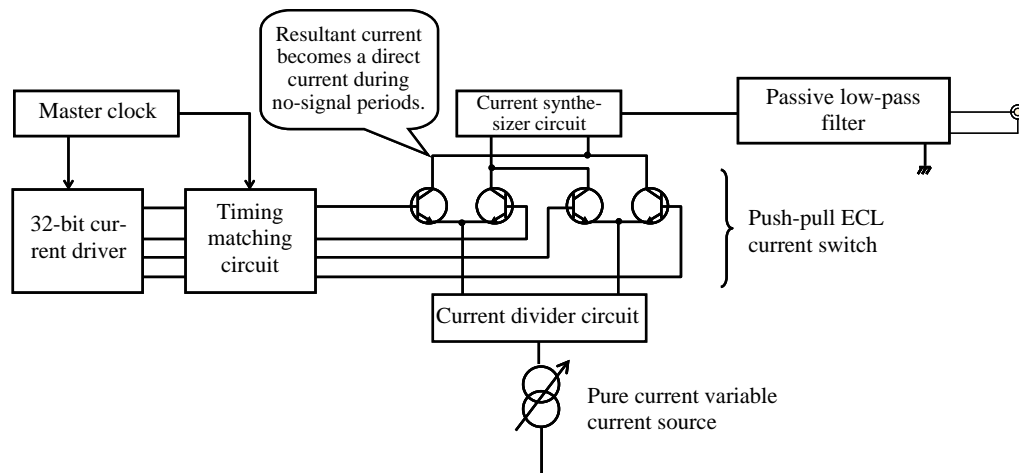


Fig. 3 Configuration of pure variable current D/A converter

passive circuit is employed without using any amplification circuit, to produce extremely direct, high-definition sound.

Figure 4 shows the passive low-pass filter circuit for the current-to-voltage conversion, which is configured with a third-order LCR filter.

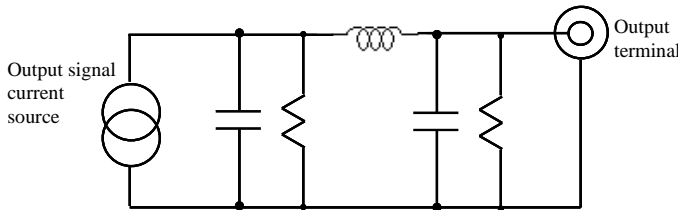


Fig. 4 Passive low-pass filter circuit for current-to-voltage conversion

3.2 Pure Digital Isolator

In digital audio devices, digital noise and jitter generated before the digital signal processing stage are very difficult to block from entering the D/A converter through the power supply or ground line. To solve this problem, in the DA-PX1, the transformer windings in each circuit block are completely separated from the power supply and ground lines; also, pure digital isolators are inserted to thoroughly block the digital noise and jitter from being transmitted from the DSP to the D/A converter (Fig. 5).

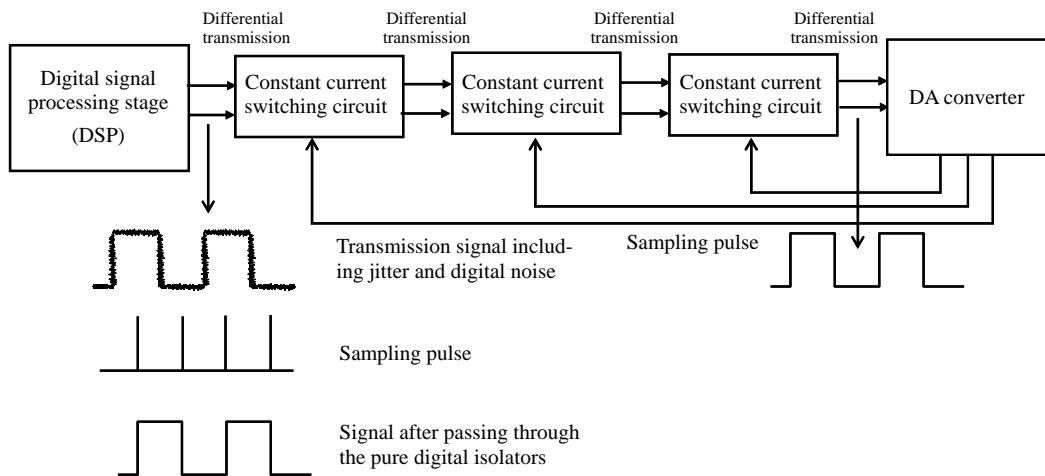


Fig. 5 Pure digital isolator

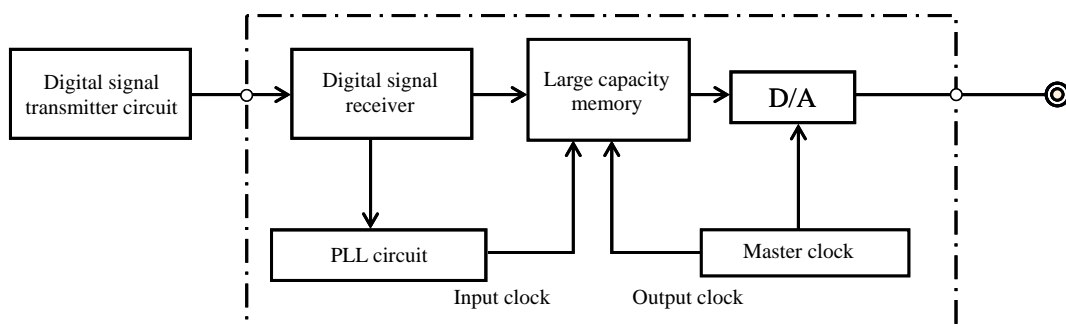


Fig. 6 Memory time corrector system

Any influences coming from the operation of surrounding circuits are completely blocked by operating the constant current switch, which has no effect on the power supply or ground line, and employing the digital balanced differential transmission between the DSP and D/A converter to block any digital noise caused by the transmission.

3.3 Two Types of Time Base Corrector

3.3.1 Memory Time Corrector

The difference in the clock timing between the transmission and reception side is very small at about 100 ppm (about one time every 10,000 samplings). Therefore, if the time delay operation is performed by using memory capacity sufficient for storing the data for, e.g., one second, a transmitter-to-receiver clock error in about 2.8 hours can be absorbed. By doing this, the DAC part is operated with the master clock, which is separated from the transmitter side and thus not affected by the jitter. At the same time, the DAC uses the transmitted data as it is. Consequently, although this system operates in an asynchronous digital transmission mode, it achieves performance and sound quality equivalent to that of the ideal synchronous transmission system. This "memory time corrector" unit has been

implemented in our system for the first time as an automotive application (Fig. 6).

3.3.2 Real-Time Corrector

The memory time corrector is the closest to the ideal as an asynchronous digital transmission system. However, it is not applicable to AV system where a time difference between transmission signals and reproduction signals occurs and no time delay is allowed. Therefore, considering that a clock difference between the transmitter and receiver occurs only at a very low frequency of about 100 ppm or less, we developed a real-time corrector, an asynchronous real-time jitter absorbing technology (Fig. 7). In this system, the D/A converter is operated with the master clock, which is separated from the transmitter side and thus not affected by the jitter; at the same time, while most data from the DAC is used as it is, when a clock difference occurs, a small amount of data is inserted or removed. The data for insertion or removal is selected by using our own automatic detection algorithm so that the sound quality is least deteriorated for the sense of hearing, thus maintaining a high sound quality. This system prevents any transmission jitter and achieves real-time properties.

4. Conclusion

Digital audio has a history of more than a quarter century since the audio CD was first introduced. However, even if the same data is used, the sound quality may still change due to the difference in the transporter or type of media, or when the CD is copied to a CD-R. Compared with the conventional system, when the same data is used, the DA-PX1 has successfully compressed the difference in the sound quality caused by the difference in media and other factors. In addition, the digital flavor in the sound is almost completely eliminated. While digital audio still has considerable room for improvement, we hope that the DA-PX1 contributes to part of this improvement.

References

- (1) Isao Shibasaki: "Progress of Digital Audio in 30 Years", No. 43, D/A Converter (No. 8), "Constant current type one-bit DAC that is highly appreciated for the sound quality"; Musen to Jikken (Audio Technology), No. 1043, 108–115 (2010)
- (2) Hiroshi Wakimori: "Great Revolution for Car Audio! DIATONE DA-PX1", Auto Sound, 68, 56–59 (2009)

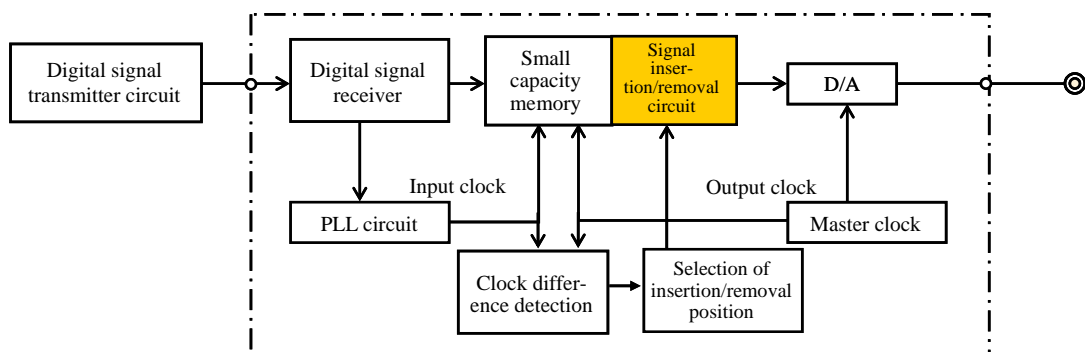


Fig. 7 Real-time corrector system

Third-Generation Power Unit for HEVs

Authors: Takuya Michinaka* and Yuji Kuramoto*

1. Introduction

The diversity of hybrid electric vehicles (HEVs) requires that the integrated intelligent power drive unit (IPU) carry specifications in accordance with a mild or full hybrid system. To meet these needs, we have developed a third-generation IPU product lineup: the high-performance 3G-IPU for mild HEVs; and the high-power 2GM-IPU for full HEVs. The 2GM-IPU covers high-voltage, high-current specifications and the 3G-IPU focuses on functional integration and compact size.

2. Technologies Applied to the IPU for Full HEVs

The 2GM-IPU (600 A and 300 A) is a compact IPU with a built-in boost converter power module, suitable for full HEVs carrying high-voltage, high-current specifications (900 V, 600 A). Figure 1 shows the configuration of this IPU. Two units of the 300-A rated transfer-molded power module (T-PM) are used in parallel to achieve the rating of 600 A. Since the IPU is mounted inside the transmission, it requires high vibration-proof like the existing model.

Challenges for satisfying these requirements are:

- (1) Parallel drive operation of T-PMs
- (2) Compact outline and vibration-proof structure

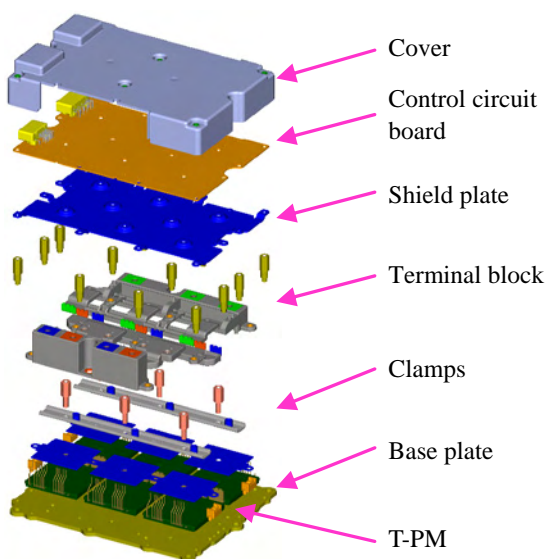


Fig. 1 Internal structure of the IPU for full HEV (2GM-IPU 600 A)

2.1 Parallel Drive Operation of T-PMs

When the power chips in the two T-PMs are driven in parallel, a current imbalance may cause a problem. Therefore, the main circuit and control board must be optimally designed to match the characteristics of the parallel drive chips, low inductance, and symmetric wiring.

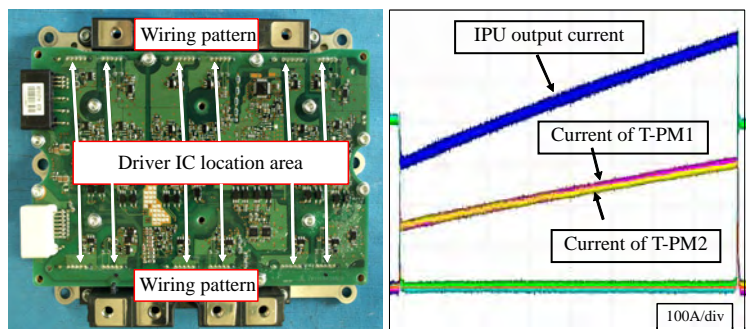
In the parallel drive circuit for this IPU, as shown in Fig. 2 a), the driver ICs are arranged in the middle of the control circuit board and the wiring is arranged symmetrically with respect to the control terminals of each pair of parallel driven T-PMs. In addition, the bus bars of the main circuit are arranged and connected to ensure wide parallel plates and thus reduce inductance.

With these measures, as shown in Fig. 2 b), the parallel drive current is equally distributed through the two T-PMs.

2.2 Vibration-resistant Structure

Since this IPU is mounted inside the transmission, it must be vibration-proof from the low-frequency to high-frequency region. However, although a multipoint fastening structure was employed to hold the control circuit board, high acceleration was forced due to resonance vibrations. As a countermeasure, each component must tolerate sufficient acceleration to satisfy the reliability specifications, and the holding structure was reinforced in the area where low vibration-proof components (mainly large components) are mounted (Fig. 3).

In the area where the power supply transformer is mounted, a special holder was attached to support the control circuit board directly from the base plate, and in



a) Control circuit board

b) Current waveform

Fig. 2 Drive circuit for parallel operation (2GM-IPU 600 A)

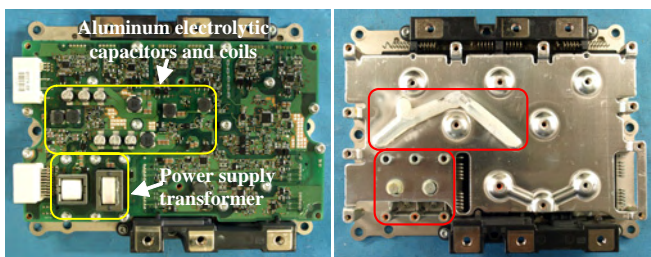
the area where aluminum electrolytic capacitors and coils are mounted, the critical damping ratio was increased by bonding the control circuit board to the shield plate.

Figure 4 shows the resonance waveforms in the object area before and after the countermeasures. These countermeasures reduced the acceleration response factor to about one-quarter, clearing the acceptance level for the parts to be mounted.

3. IPU Technologies for Mild HEVs

The 3G-IPU was developed for mild HEV systems, focusing on the compact size, light weight and low cost required for these systems.

The configuration of this IPU is shown in Fig. 5.



a) Location of large-size components mounted on the control circuit board
 b) Countermeasure for the structure holding the control circuit board

Fig. 3 Countermeasures for vibration resistance (2GM-IPU 300 A)

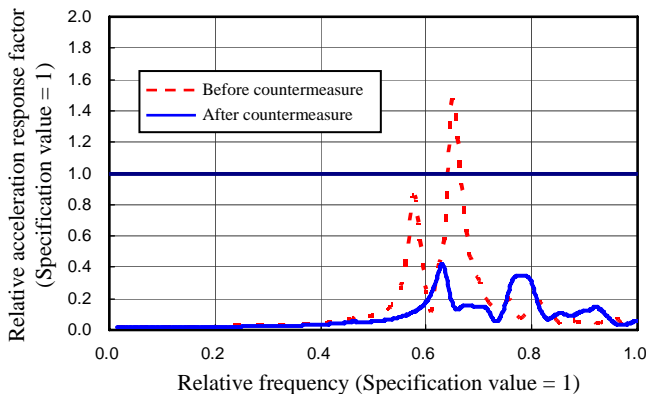


Fig. 4 Effect of countermeasures for vibration resistance (2GM-IPU 300 A)

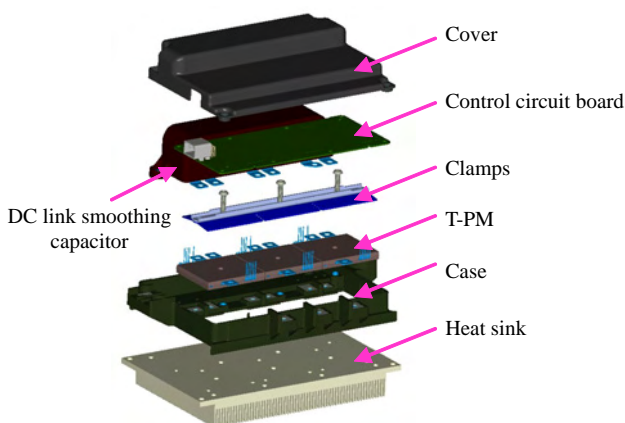


Fig. 5 Internal structure of the IPU for mild HEV

Like the second-generation IPU (2G-IPU), the 3G-IPU has a built-in DC link smoothing capacitor and heat sink for inverter operation, and a build-up structure to facilitate assembly.

Table 1 shows the effects of developing the 3G-IPU.

Table 1 Effects of developing the 3G-IPU for mild HEV

Approach	Related components	Effect	Compact size	Light weight	Low cost
Speedup of overvoltage protection	DC link smoothing capacitor	Lower capacitance	○	○	○
	Heat sink	Lighter weight	○	○	○
DLB structure	T-PM	Smaller chip size			○
		Improved productivity			○

3.1 Speedup of Overvoltage Protection

The IPU is protected from overvoltage generated across the DC link smoothing capacitor by abnormal regenerative power from the three-phase motor. Figure 6 shows the operation time for overvoltage protection vs. percent reduction in the capacitance of the DC link smoothing capacitor. The response time of the overvoltage protection is dependent on the time of voltage detection by the microprocessor in the IPU, and the amount of voltage increase is dependent on the capacitance of the DC link smoothing capacitor.

By raising the clock speed of the microprocessor and improving the sampling method, the operation time for overvoltage protection was halved and thus the capacitance of the DC link smoothing capacitor was also halved. Along with the reduction in capacitance, the DC link smoothing capacitor could be made smaller; in addition, the weight of the heat sink was also reduced to 60%, on which the DC link smoothing capacitor is mounted.

With these effects, the 3G-IPU is 30% smaller, 40% lighter, and more than 40% cheaper than the 2G-IPU.

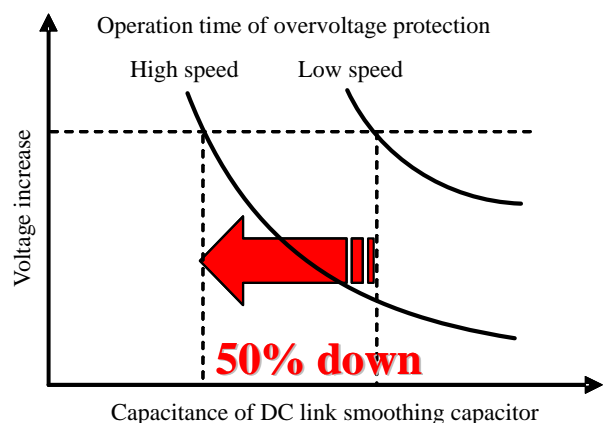


Fig. 6 Range of overvoltage protection

3.2 DLB Type T-PM

In the T-PM, which is installed in all third-generation IPU models, as shown in Fig. 7, the wire connection to the power chips is made by direct lead bonding (DLB) instead of wire bonding (WB) used for the second-generation IPU.

The DLB method increases the wire current density and thus achieves a smaller power chip size and higher productivity, resulting in lower production cost. It also reduces internal impedance, and improves endurance and performance. We have developed and begun mass production of the third-generation IPU lineup: the higher power output 2GM-IPU for full HEVs, and the compact 3G-IPU for mild HEVs.

References

- (1) Yuji Kuramoto, et al.: "2nd Generation IPU for HEV", Mitsubishi Denki Giho 81, No. 9, 581–584 (2007)
- (2) Akinori Akazawa, et al.: "Development of Transmission Built-in Type IPU", Mitsubishi Denki Giho 78, No. 9, 569–572 (2004)
- (3) Kazuhiro Tada, et al.: "Molding Technology for Power Modules", Mitsubishi Denki Giho 78, No. 11, 743–746 (2004)

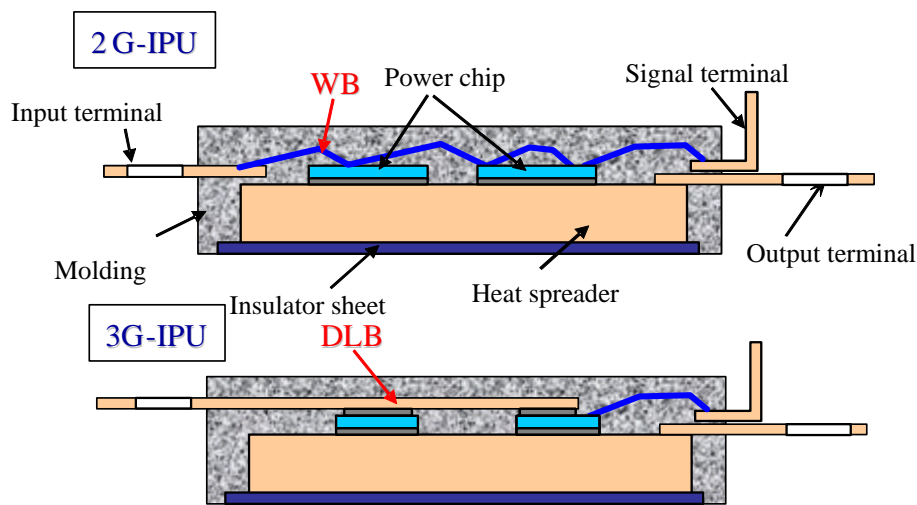


Fig. 7 Comparison of internal structures of T-PM

Estimation of Maximum Tire-Road Friction Coefficient Using Electric Power Assist Steering

Authors: Fumiaki Takagi* and Noriyuki Inoue**

1. Introduction

In general, on a snow-covered or otherwise slippery road, an abrupt steering change will cause unstable vehicle behavior, or excessive speed will make the vehicle deviate from the intended path. The vehicle stability control (VSC) system detects such conditions and stabilizes the vehicle. Although the use of VSC has begun to increase, it is not yet widely seen in inexpensive cars, partly because of its high cost. This paper proposes a low-cost method for estimating the tire-road friction coefficient using only standard signals from the sensors installed in the electric power assist steering (EPAS) system.

2. Method for Estimating Tire-Road Friction Coefficient

When making a turn, the reaction given to the steering wheel varies depending on the vehicle speed, steering wheel angle and road surface conditions. The tire-road friction coefficient can be estimated from this feedback reaction, simply by detecting a road surface-derived component using the EPAS system. The principle of this detection method is described below with the relevant background.

2.1 Fiala Tire Model

The Fiala tire model is well known for explaining the side force exerted on the tire⁽¹⁾. The direction of the tire's rolling motion seemingly coincides with the actual direc-

tion of travel. However, there is a slight difference when the vehicle is going around a curve or during similar situations. The Fiala tire model demonstrates how the angle between the two directions generates a side force on the tire. This angle is called the "tire sideslip angle", and the dimensionless quantity converted from this sideslip angle with correction for the influence from the load, the tire's own gripping property, and other factors is called the dimensionless sideslip angle, ψ .

According to the Fiala tire model, if the dimensionless sideslip angle ψ is increased by turning the steering wheel, as shown in Fig. 1, the tire side force F gradually increases up to the limit of the friction, whereas the tire self-aligning torque M , which makes the tire turn about the tire center axis, saturates at a certain angle and then decreases.

2.2 Influence of Steering Wheel

It should be noted that the torque M of the Fiala model does not correspond to the reaction given to the steering wheel. In the actual steering system, as shown in Fig. 2, the kingpin axis is inclined from the tire's center axis, and thus the self-aligning torque about the kingpin, M_z , which corresponds to the reaction given to the steering wheel, differs from the torque M , where the "kingpin axis" refers to the axis around which the tire is turned by the steering wheel.

Mitsubishi Electric has conducted extensive research on the torque about the kingpin axis

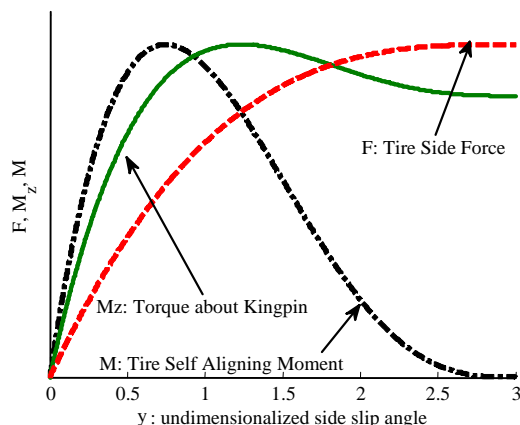


Fig. 1 Fiala Model

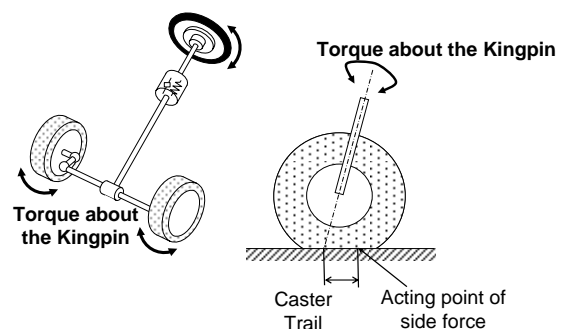


Fig. 2 Schematic drawing of steering system

(self-aligning torque) that indicates the reaction given to the steering wheel, and found that this torque also has a local maximum value similar to the tire self-aligning torque M , and the local maximum value is proportional to the tire-road friction coefficient (Fig. 3).

By detecting this local maximum value and using the proportionality relationship, the tire-road friction coefficient can be estimated.

2.3 Estimation of Self-Aligning Torque

The self-aligning torque is obtained by considering the balance between the forces acting on the steering system. That is, the self-aligning torque is estimated based on the sum of the steering torque given by the driver and the torque assisted by the EPAS. In this estimation, signal processing is performed to remove noises⁽²⁾.

2.4 Detection of Local Maximum Value of Self-Aligning Torque

Under normal conditions, the local maximum value of the self-aligning torque should be detected by the maximum condition on the dimensionless sideslip angle ψ . Instead, the maximum condition on the steering wheel angle θ is used for the detection, because this reduces the number of sensors. It should be noted, however, that a slight correction is added to avoid any erroneous detection of the local maximum value due to external disturbances on the road⁽³⁾.

2.5 Self-Aligning Torque Conversion Coefficient

The proportionality relationship between the local maximum value of the self-aligning torque about the kingpin, M_{zmax} , and the tire-road friction coefficient μ is expressed by:

$$M_{zmax} = \frac{1}{512l^3} (l + 6\xi_c)(27l^3 + 134l^2\xi_c - 156l\xi_c^2 + 72\xi_c^3)W\mu \quad (1)$$

where l is the tire contact length, ξ_c is the caster trail, and W is the tire vertical load.

This relationship was verified using an actual car: the verification result (Fig. 4) shows that the proportion-

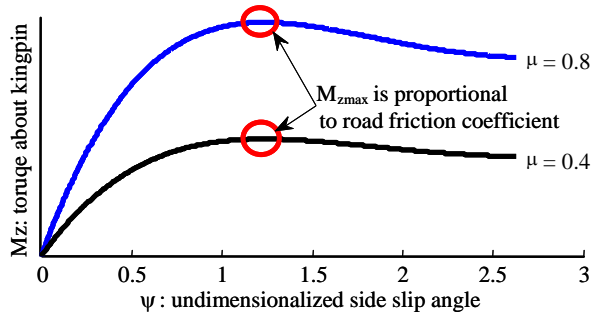


Fig. 3 Local maximum point of self-aligning torque

ality relationship holds true. However, the linear regression line does not pass through the origin, indicating that the actual proportionality relationship differs from Eq. (1) with a non-zero constant term, which is due to the influence of a friction component in the steering system. The value of the x-intercept corresponds to the amount of friction torque.

By reverse calculation using this relationship, the tire-road friction coefficient μ is obtained from the local maximum value of the self-aligning torque about the kingpin M_{zmax} .

2.6 Verification of Estimation Accuracy

The accuracy was verified for the proposed estimation method of the tire-road friction coefficient.

2.6.1 Estimation Accuracy under Nominal Conditions

The estimation accuracy of the tire-road friction coefficient under nominal conditions was verified under the same driving conditions used to set up the parameters described in Section 2.5 (Fig. 5). The horizontal axis represents the measured value of the tire-road friction coefficient, which was obtained from the maximum value of the lateral-acceleration sensor reading; the vertical axis represents the estimated value using the proposed method; and each point corresponds to each verification cycle. As clearly seen from the chart, the estimation error was within ± 0.1 .

2.6.2 Estimation Accuracy under Varying Vehicle Weight and Tire Conditions

The estimation accuracy was also verified under conditions different from those used to set up the parameters shown in Section 2.5 (Fig. 6). In this estimation method, the model parameters, i.e., tire contact length and tire vertical load, are set as constants, and thus when these parameters vary, there is a concern about deterioration in estimation accuracy. In this verification, as shown in Table 1, the actually changed

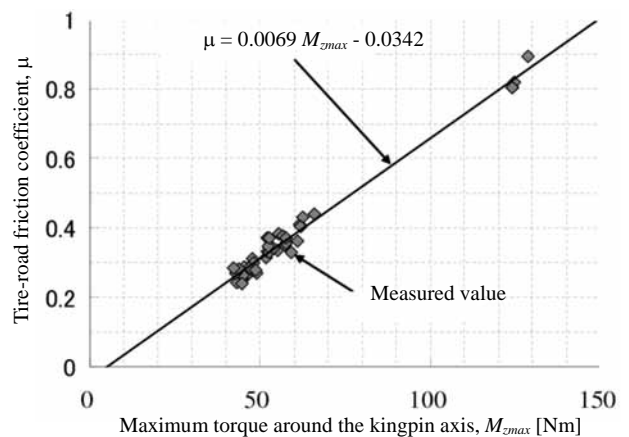


Fig. 4 Correlation between tire-road friction coefficient and self-aligning torque

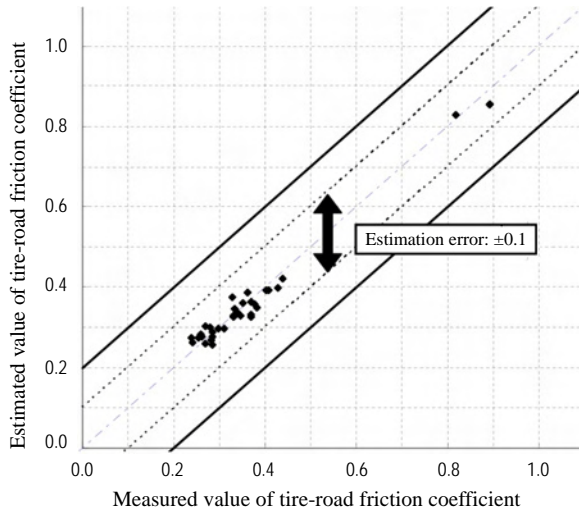


Fig. 5 Estimation accuracy under nominal conditions

variables were the tire pressure and load conditions, which could alter the model parameters. Under Condition A, the estimated value of the tire-road friction coefficient becomes smaller than the measurement; whereas under Condition B, the estimated value becomes greater than the measurement. It was confirmed that even though the estimation error increases in these cases, the increase remains within about ± 0.2 .

Table 1 Test Conditions

	Load	Tire pressure
Nominal conditions	Driver only	220 [kPa]
Condition A	Driver only	300 [kPa]
Condition B	300 [kg]	150 [kPa]

3. Conclusion

We have proposed a method for estimating the tire-road friction coefficient, which uses the proportionality relationship between the tire-road friction coefficient and the maximum value of the self-aligning torque about the kingpin.

The proposed method enables the detection of the maximum value of the self-aligning torque using only the electric power assist steering system, without any additional sensors such as acceleration, yaw rate and steering wheel angle sensors. Also, the computational load is low, resulting in low implementation cost.

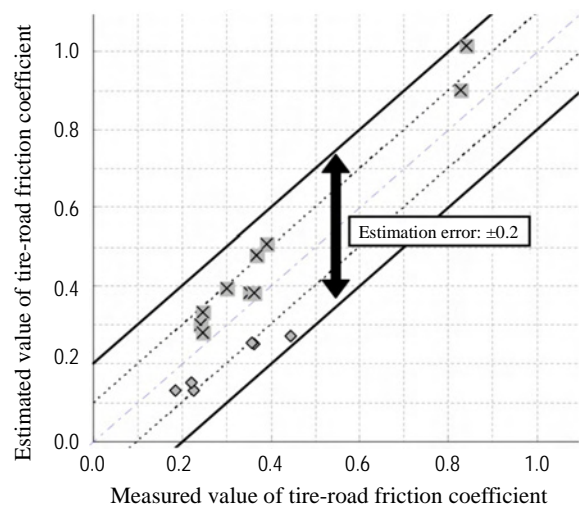


Fig. 6 Estimation accuracy under varying vehicle conditions

While we have theoretically derived the abovementioned proportionality relationship from the Fiala tire model, we have also experimentally verified the relationship. Although the proportionality coefficient in this relationship is dependent on the tire vertical load and tire contact length, even if these conditions vary, the estimated value of the tire-road friction coefficient is within ± 0.2 of the maximum value of lateral acceleration.

This estimation method will be useful for developing active safety systems.

References

- (1) E. Fiala: "Seitenkrafte am Rollenden Luftreifen", DI Zeitschrift, 96, 1954
- (2) Hideyuki Tanaka, Masahiko Kurihara, Toshihide Satake, and Takayuki Kifuku: "Improvement of Stability Using Estimated Alignment Torque for EPS", Proceedings of the Transportation and Logistics Conference, Vol. 2005, No. 14 (2005-12-06), pp. 163-166 (2004)
- (3) K. Nakajima, et al.: "A Vehicle State Detection Method Based on Estimated Aligning Torque using EPS", AVEC 2005, No. 2005-01-1265

Model-Based Development of Electronic Control Unit for 4WD

Authors: Kazuyuki Adachi* and Shinsuke Ui*

1. Introduction

Software programs (S/W) embedded in the electronic control unit (ECU) have become increasingly complex and large-scale due to several factors including more sophisticated fault diagnostic functions and more stringent regulations on vehicle fuel consumption and exhaust gas emission as countermeasures against environmental problems. As a result, the number of man-hours for development tends to increase, and so automakers have begun introducing the model-based approach to improve development efficiency.

The environment for model-based development is being established, where the S/W is developed by: describing the control specifications as an executable control flow chart called the model, performing simulations to verify the control specifications, and automatically generating source code from the model by means of generator tools. MATLAB and Simulink^(Note 1) are both well-known model development tools. In an environment where the source code is automatically generated by such tools, there is an advantage in that the man-hours for S/W development can be significantly reduced. However, it is still necessary to improve the efficiency of the S/W verification process. Mitsubishi Electric has been working on improving the verification process in model-based development. This paper presents an approach applied to the model-based development of the 4WD ECU for Mitsubishi Motors Corporation.

2. Establishment of the Verification Environment for Model-Based Development

2.1 Challenges in the Verification Process

In the verification process in model-based development, contents of the S/W are verified on the following subjects:

“Subjects of S/W verification”

Verification (1): Are the control specifications properly implemented?

Verification (2): Does the fixed-point arithmetic processing provide sufficient computational precision?

First, Verification (1) is described. The model that describes the vehicle control is diverse in terms of the

contents, scale, etc., making it difficult to ensure that the tools will generate fault-free source code for all models. Therefore, each time the tools automatically generate source code from the model, the generated code must be checked for errors.

Next, Verification (2) is described. In Mitsubishi Electric’s S/W, a physical quantity is represented by a one-bit decimal fixed-point number and an unsigned integer with an offset. In the model, a physical quantity is represented by a double-precision floating-point number, using eight bytes of memory; whereas the fixed-point format uses only two bytes each (in the case of the ECU for 4WD). If physical quantities are represented in the fixed-point format, the size of the memory for the S/W is reduced and it is easier to implement the S/W on an inexpensive microprocessor with less memory. However, the fixed-point representation of physical quantities could create a loss of precision during S/W calculations. As a consequence, it is necessary to only partially use the fixed point, by carefully considering the computational precision required by the S/W’s control specifications (referred to as the tolerance hereinafter), and by checking if the computational precision is affected and outside the tolerance.

2.2 Development of “MC-Checker”

Since 2007, to improve the verification process in model-based development, Mitsubishi Electric and tools provider Gaio Technology Co., Ltd. have jointly conducted the specification design and development of “MC-Checker”, a tool for checking the compatibility between the model and the S/W. MC-Checker has two main functions, as shown in Fig. 1:

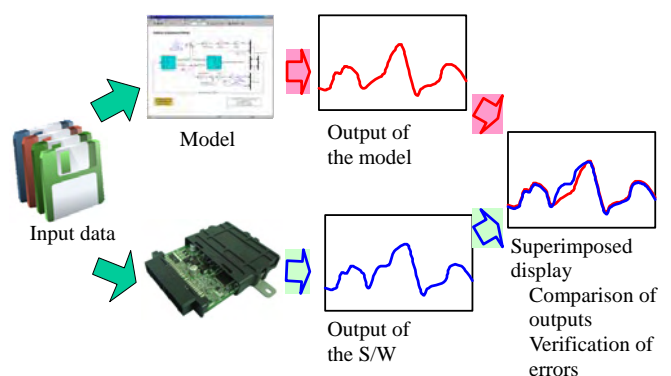


Fig. 1 Functions of MC-Checker

Note 1 MATLAB and Simulink are trademarks of MathWorks, Inc., USA.

Function (1): Comparison of outputs from the model and the S/W.

This function, on a personal computer, provides both the model and the S/W with the same input data, performs a simulation of each system, and displays a graphical comparison of the outputs from the model and the S/W.

Function (2): Detection of S/W output exceeding the tolerance.

On the chart comparing the outputs from the model and the S/W obtained in Function (1), this function detects and marks the position where the output from the S/W is outside the tolerance range, which has been set by the user with respect to the model output. This function enables the user to visually confirm at a glance that the output from the S/W is within the tolerance.

2.3 Application to the Model-Based Development of ECU for 4WD

This section presents a case example of the newly developed MC-Checker applied to the model-based development of the 4WD control system for Mitsubishi Motors Corporation.

The 4WD control system called S-AWC or Super-All Wheel Control^(Note 2) consists of, as shown in Fig. 2, the ECU for S-AWC, the electronic control 4WD that distributes the driving force between the front and rear axles, and the active front differential (AFD) that distributes the driving force between the left and right front wheels. The ECU for S-AWC collectively controls the front electronic control coupling (F-ECC) for the AFD,

and the center electronic control coupling (C-ECC) for the electronic control 4WD. The ECU for S-AWC achieves high driving performance by obtaining information, from various sensors and other ECUs through CAN communications, on the vehicle driving conditions such as the steering angle, wheel speed, and front and rear acceleration. Based on these driving conditions, the ECU controls the engaging torque in the ECCs to distribute the driving force between the left and right front wheels as well as between the front and rear axles.

The MC-Checker was used to compare the outputs for the F-ECC provided by the model and the S/W. Figure 3 shows the results: a significant difference was found in a certain area, revealing a problem in the S/W.

The cause analysis revealed that the state transition variables of the model and S/W are assigned with values tabulated in Table 1, indicating a difference in the handling of oversteer.

Table 1 Variables representing vehicle state transition

State of vehicle	Value of variable for determining state transition	
	Model	S/W
Understeer	1	1
Straight	0	0
Oversteer	-1	-

After correcting the difference in handling the state transition variable, the outputs for the F-ECC provided

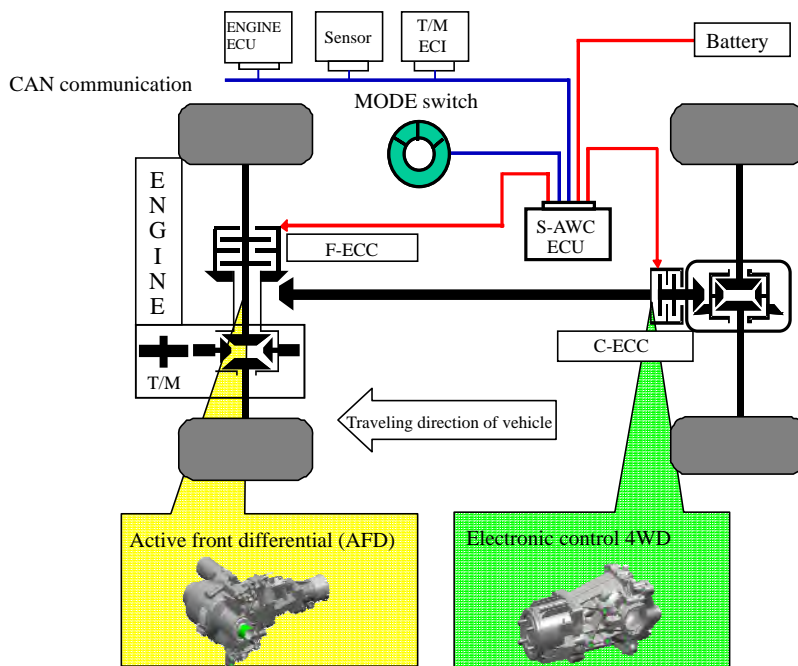


Fig. 2 4WD control system

Note 2 S-AWC is a registered trademark of Mitsubishi Motors Corporation.

by the model and the S/W were compared again. The result is shown in Fig. 4. The output of each F-ECC is nearly equal, thus confirming proper operation of the S/W.

2.4 Improvement of the Computational Precision of the S/W

Function (2) of the MC-Checker was used to detect an output of the S/W exceeding the tolerance. As shown in Fig. 5, a difference greater than the tolerance of 1 Nm was detected in the S/W output for the C-ECC. It was found that the arithmetic processing of a fixed-point map created a large difference between the outputs from the model and the S/W.

A fixed-point map is a fixed-point data array representing inflection points extracted from a chart showing the relationship between the input and output values of a certain physical quantity. In the arithmetic processing

of fixed-point maps, when an input value is given, a search operation is carried out for the interval between two inflection points into which the input value falls, and then an interpolation is made to calculate the output value.

A large variance was found in the output with respect to the input value within the interval on the fixed-point map where an interpolation is calculated, resulting in coarse precision of the interpolation calculation. Therefore, the arithmetic processing of fixed-point maps was improved so that, within the interval where an interpolation is calculated, any variance in the output with respect to the input value always becomes smaller than the limit of resolution of the output. After the improvement, the outputs from the model and the S/W were compared again. The result is shown in Fig. 6: the output for the C-ECC provided by the S/W always falls within the limit of the tolerance of 1 Nm.

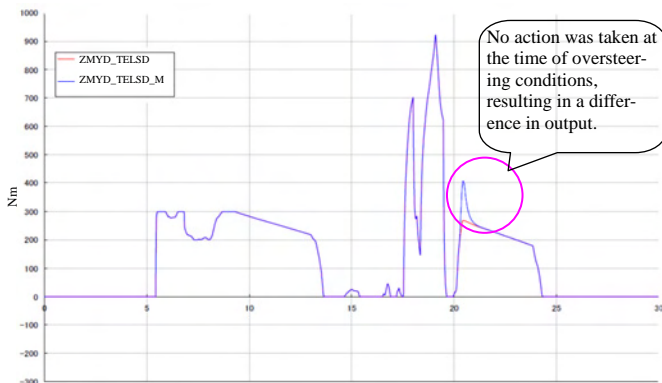
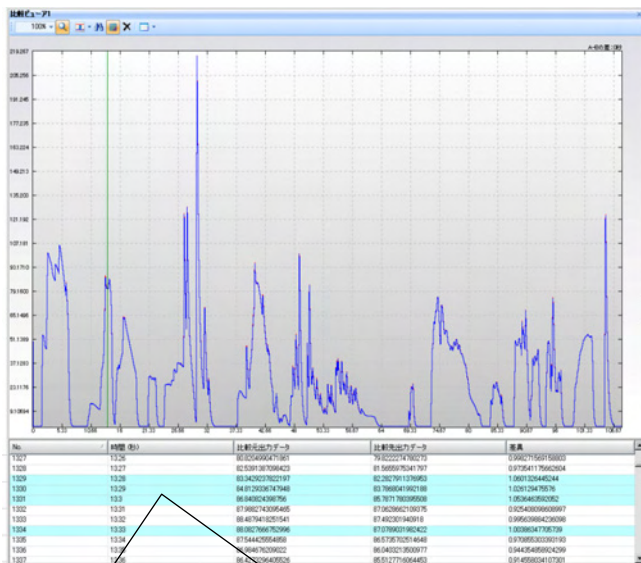


Fig. 3 Comparison of outputs for F-ECC (before correction)

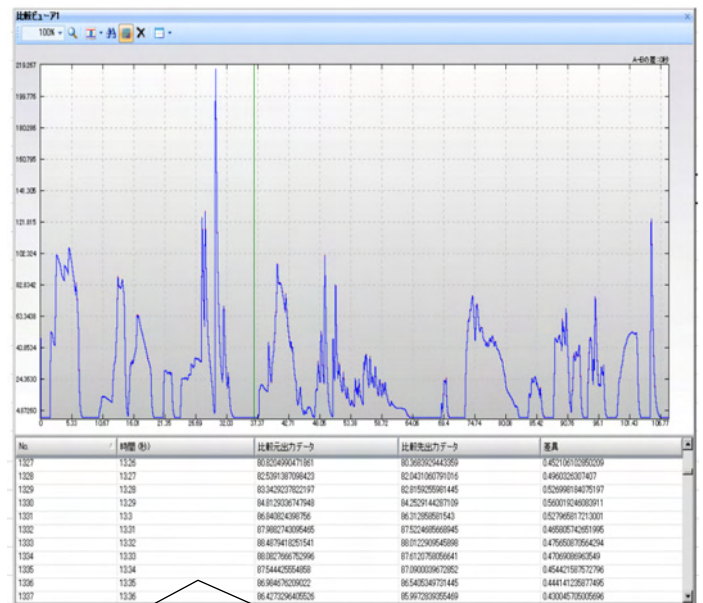


Fig. 4 Comparison of outputs for F-ECC (after correction)



On the time-series data and the graphical output, markings are displayed at positions where the difference is 1 Nm or greater.

Fig. 5 Detection of output for C-ECC exceeding the tolerance (conventional)



There are no positions where the difference is 1 Nm or greater, and thus no markings are displayed.

Fig. 6 Detection of output for C-ECC exceeding the tolerance (after improvement)

3. Conclusion

As described above, the newly developed MC-Checker improves the efficiency of verification in model-based development. In future, we intend to add processing time measurement and other functions to the MC-Checker to deal with restrictions of the micro-computer other than the limited amount of memory.

References

- (1) Yuji Kuramoto, et al.: "2nd Generation IPU for HEV", Mitsubishi Denki Giho 81, No. 9, 581–584 (2007)
- (2) Akinori Akazawa, et al.: "Development of Transmission Built-in Type IPU", Mitsubishi Denki Giho 78, No. 9, 569–572 (2004)
- (3) Kazuhiro Tada, et al.: "Molding Technology for Power Modules", Mitsubishi Denki Giho 78, No. 11, 743–746 (2004)

